J|A|C|S
COMMUNICATIONS

Published on Web 06/01/2006

Off-Resonance TROSY-Selected $R_{1\rho}$ Experiment with Improved Sensitivity for Medium- and High-Molecular-Weight Proteins

Tatyana I. Igumenova and Arthur G. Palmer, III*

Department of Biochemistry and Molecular Biophysics, Columbia University, New York, New York 10032

Received March 10, 2006; E-mail: agp6@columbia.edu

Solution NMR techniques, such as Carr−Purcell−Meiboom−Gill (CPMG), Hahn spin−echo (HE), and $R_{1\rho}$ experiments, are powerful approaches for site-resolved characterization of dynamic processes in macromolecules on biologically relevant time scales, as demonstrated by recent studies of protein folding, catalysis, and allosteric phenomena (for reviews, see ref 1). These methods measure the contribution of chemical exchange, R_{ex}, to the phenomenological relaxation rate constant in the transverse or tilted rotating frames; however, R_{ex} is independent of protein size and consequently makes a smaller fractional contribution to relaxation in larger proteins. *T*ROSY-selected (TS) experiments, such as the TS−CPMG[2] and TS−HE[3] pulse sequences, alleviate this problem by measuring the contribution of R_{ex} to the slowly relaxing or narrow TROSY[4] component of a *J*-coupled multiplet. The $R_{1\rho}$ experiment is the most versatile of the three techniques because both the amplitude, ω_1, and resonance offset, Ω, of the spin-lock field are under experimental control;[5] consequently, lack of a TS version has hindered progress in understanding protein conformational dynamics.

Here, we present an off-resonance TS−$R_{1\rho}$ experiment for quantifying microsecond time scale chemical exchange in [^{2}H, ^{15}N]-enriched proteins. The pulse sequence for the TS−$R_{1\rho}$ experiment, shown in Figure 1A, selectively creates and maintains the ^{15}N TROSY component, resulting from destructive relaxation interference between ^{15}N chemical shift anisotropy (CSA) and ^{1}H−^{15}N dipole−dipole (DD) interactions in amide groups of the protein backbone, throughout the relaxation delay, *T*, and the evolution period, t_1. During the preparation period, antiphase coherence H_zN_y generated by the INEPT sequence (point **a**) is converted to $H^\beta N_z$ by the S^{3}E filter[6] (point **b**). Relaxation in the tilted rotating frame occurs during two spin-lock periods separated by the S^{3}CT selective-inversion element.[7] During each spin-lock period, $H^\beta N_z$ is aligned along the effective field by an adiabatic ramp, generating $H^\beta N_z'$ coherence,[8] allowed to relax for *T*/2, and returned to the laboratory frame *z*-axis by a time-reversed adiabatic ramp. After the relaxation period (point **c**), $H^\beta N_z$ is rotated to the transverse plane and a two-dimensional ^{1}H−^{15}N chemical shift correlation spectrum is recorded using the sensitivity- and gradient-enhanced TROSY sequence.[9] The longitudinal, transverse, and tilted rotating frame relaxation rate constants for the relevant $H^\beta N_z$, $H^\beta N_-$, and $H^\beta N_z'$ operators, respectively, are given by

$$R_1^\beta = R_1 - \eta_z + \mu_{1H}$$
$$R_2^\beta = R_2^0 - \eta_{xy} + \mu_{1H} + R_{ex} = R_2^{\beta,0} + R_{ex}$$
$$R_{1\rho}^\beta = R_1^\beta \cos^2\theta^\beta + R_2^\beta \sin^2\theta^\beta \qquad (1)$$

in which R_2^0 (R_1) is the transverse (longitudinal) auto-relaxation rate constant for in-phase (longitudinal) ^{15}N magnetization due to ^{15}N CSA and ^{15}N−^{1}H DD relaxation mechanisms, η_{xy} (η_z) is the transverse (longitudinal) ^{15}N CSA/^{15}N−^{1}H DD relaxation interference rate constant, μ_{1H} is the relaxation rate constant due to the DD interactions of ^{1}H^N with remote ^{1}H spins, $\theta^\beta = \arctan(\omega_1/\Omega^\beta)$ is the tilt angle of the effective spin-lock field, and $\Omega^\beta = \Omega + \pi J$. Contributions of ^{1}H−^{15}N DD cross-relaxation and ^{1}H CSA interactions to $R_{1\rho}^\beta$ are negligible for large proteins.

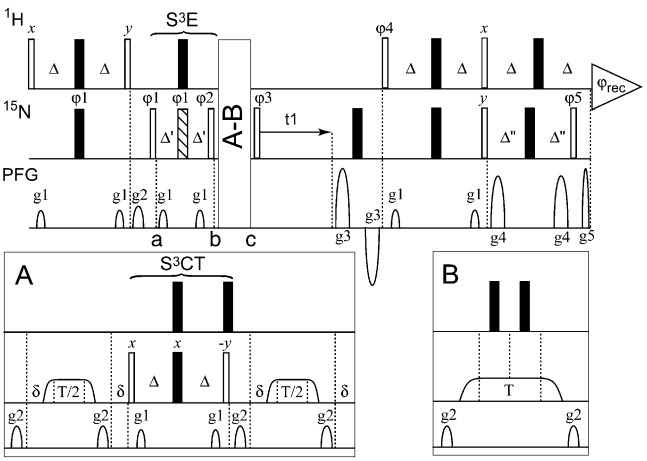

Figure 1. Off-resonance (A) TS−$R_{1\rho}$ and (B) $R_{1\rho}$−TD pulse sequences. In (A), δ is set to zero for conventional or to $(T_{max} - T)/4$ for CRT[12] versions of the TS−$R_{1\rho}$ experiment. T_{max} is the maximum duration of the relaxation delay *T*, $\Delta = 2.7$ ms, $\Delta' = 1.30$ ms, and $\Delta'' = 2.49$ ms. Empty and filled bars indicate 90 and 180° pulses, respectively. The hatched bar corresponds to a composite $90_y°-180_x°-90_y°$ pulse. The last ^{1}H 180° pulse is either a rectangular or a 3−9−19 pulse.[13] The ^{1}H carrier frequency is centered in the amide region between points b and c and is set on the water resonance during other parts of the sequence. The phase cycle is $\varphi_1 = 4(x, -x)$, $\varphi_2 = 4(135°)4(315°)$, $\varphi_3 = 2(y, y, -y, -y)$, $\varphi_4 = -y$, $\varphi_5 = -x$, and $\varphi_{rec} = (x, -x, -x, x, -x, x, x, -x)$. The phases are specific to Bruker spectrometers; for Varian spectrometers, *y*-phases should be inverted. Gradient pulses are sine-shaped and have the following durations and amplitudes: $g_1(z) = 0.5$ ms, 6 G/cm; $g_2(z) = 1.0$ ms, 10 G/cm; $g_3(z) = 0.9$ ms, 28 G/cm; $g_4(xyz) = 1$ ms, 20 G/cm; $g_5(xyz) = 0.182$ ms, 28 G/cm. In (B), the S^{3}E element is converted to a refocused INEPT sequence by setting $\Delta' = 2.7$ ms and $\varphi_2 = 4(y, -y)$; equilibrium ^{15}N magnetization is destroyed prior to the start of the sequence by a 90° pulse followed by a gradient pulse (not shown).

For comparison, a *T*ROSY-*d*etected $R_{1\rho}$ ($R_{1\rho}$−TD) pulse sequence, based on the CRT $R_{1\rho}$−TD experiment[10] with a modified decoupling strategy,[11] is shown in Figure 1B. The $R_{1\rho}$−TD experiment records the decay of in-phase ^{15}N magnetization during *T* and uses the TROSY sequence for detection only. Consequently, the relaxation rate constant is given by $R_{1\rho} = R_1 \cos^2\theta + (R_2^0 + R_{ex})\sin^2\theta$, where $\theta = \arctan(\omega_1/\Omega)$.

Cross-relaxation between slowly and rapidly relaxing doublet components in the tilted rotating frame, which otherwise impedes accurate measurement of $R_{1\rho}^\beta$, is suppressed effectively by (i) deuteration of nonexchangeable protein sites to reduce μ_{1H}, (ii) selective excitation of the slowly relaxing doublet component using the S^{3}E sequence to ensure that the initial amplitude of the rapidly

10.1021/ja061692f CCC: $33.50

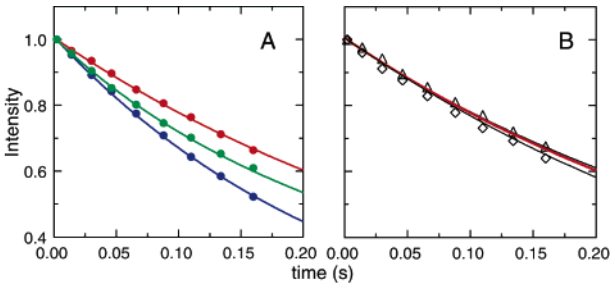

Figure 2. $R_{1\rho}$ relaxation decay curves for A28 collected with a spin-lock field strength $\omega_1/2\pi = 1768$ Hz and tilt angles $\theta = 30.3°$ and $\theta^\beta = 30.4°$. The experimental data and numerical simulations (see Supporting Information for details) are shown with symbols and solid lines, respectively. In (A), the TS$-R_{1\rho}$ (red) and $R_{1\rho}-$TD (blue) data are contrasted with the relaxation decay curve obtained using the TS$-R_{1\rho}$ sequence without S^{3}CT and S^{3}E elements (green). In (B), the TS$-R_{1\rho}$ simulation (red line) is contrasted with the data obtained without selective excitation (diamonds) and without inversion in the middle of the spin-locking period (triangles).

relaxing component is zero, and (iii) selective inversion of one of the ^{15}N doublet components using the S^{3}CT sequence to refocus cross-relaxation to first order.[14] In contrast, only (i) and (iii) are necessary to suppress cross-relaxation for purely transverse coherence in the TS$-$CPMG[2] and TS$-$HE[3] experiments.

As a model system, we chose [90%-^{15}N, 70%-^{2}H] ubiquitin, a 76-residue protein, whose hydrodynamic properties at 280 K are similar to those of a ~19 kDa protein at 308 K. As a result, ubiquitin displays an appreciable TROSY effect even at a relatively modest magnetic field strength of 500 MHz. Chemical exchange behavior of ubiquitin at 280 K, characterized previously using conventional $R_{1\rho}$ methods,[15] provides a reference for validation of the TS$-R_{1\rho}$ experiment.

Figure 2 highlights the importance of selective excitation and inversion in TS$-R_{1\rho}$, using as an example the relaxation decay curves for A28, a residue that does not exhibit chemical exchange line broadening. As shown in Figure 2A, if the S^{3}E and S^{3}CT elements are removed from the TS$-R_{1\rho}$ sequence, then the resulting relaxation decay curve (green) contains an appreciable contribution from the cross-relaxation between the slowly and rapidly relaxing ^{15}N doublet components. This contribution results in overestimation of $R_{1\rho}^\beta$, especially at small angles θ^β, where the contribution of R_1^β to $R_{1\rho}^\beta$ is relatively large. Figure 2B shows that either selective inversion or excitation substantially suppresses cross-relaxation, but both elements are needed to achieve complete suppression. Numerical simulations (Supporting Information) indicate that TS$-R_{1\rho}$ is applicable to backbone amide moieties in proteins with molecular weights at least up to 50 kDa.

Figure 3 compares TS$-R_{1\rho}$ (red) and $R_{1\rho}-$TD (blue) relaxation dispersion curves for two exchange-broadened residues in ubiquitin, I23 and N25. TS$-R_{1\rho}$ and $R_{1\rho}-$TD data are fitted accurately using the same chemical exchange parameters,[15] indicating that the cross-relaxation between slowly and rapidly relaxing ^{15}N doublet components is completely suppressed in the TS$-R_{1\rho}$ experiment. The same results hold for the other two exchange-broadened residues in ubiquitin, V70 and T55 (Figure S1). The median values of R_2^0 and $R_2^{\beta,0}$ obtained from fitting the dispersion curves are 9.93 s and 4.72 s^{-1}, respectively. The 52% reduction in the transverse relaxation rate constants in TS$-R_{1\rho}$ compared to that in $R_{1\rho}-$TD dramatically increases the relative contribution of chemical exchange to the observed transverse relaxation rates.

In summary, the TS$-R_{1\rho}$ experiment efficiently suppresses cross-relaxation between the doublet components of spin-locked ^{15}N magnetization and allows accurate measurement of the chemical exchange contribution to the slowly relaxing doublet component.

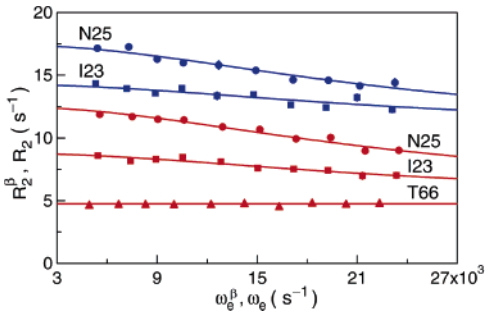

Figure 3. Relaxation dispersion curves for two exchange-broadened residues in ubiquitin, N25 (circles) and I23 (squares), collected using the TS$-R_{1\rho}$ (red) and the control $R_{1\rho}-$TD (blue) experiments. $\omega_e^{(\beta)} = (\omega_1^2 + (\Omega^{(\beta)})^2)^{1/2}$ is the strength of the effective spin-lock field. Solid lines represent the fits to the experimental data obtained using the chemical exchange parameters of Massi et al.[15] and $R_2^{\beta,0}$ (or R_2^0) as the only adjustable parameter. The $R_2^{\beta,0}$ values obtained in the TS$-R_{1\rho}$ experiment are 5.27 $\pm$ 0.05 and 5.62 $\pm$ 0.07 s^{-1} for I23 and N25, respectively, as compared to the R_2^0 values of 10.8 $\pm$ 0.1 and 10.6 $\pm$ 0.1 s^{-1} obtained in the $R_{1\rho}-$TD experiment. Representative TS$-R_{1\rho}$ relaxation dispersion curve for one of the nonexchanging residues, T66, is shown with triangles. The error bars are smaller than the symbol size.

The TS$-R_{1\rho}$ experiment completes the repertoire of TS experiments for investigation of dynamic processes on microsecond time scales in large proteins.

Acknowledgment. This work was supported by NIH Grants GM59273 (A.G.P.) and DK07328 (T.I.I.). The authors thank Clay Bracken (Cornell University) for help in preparing the ubiquitin sample, and Joel Butterwick, Francesca Massi, and Vesselin Miloushev (Columbia University) for helpful discussions.

Supporting Information Available: Relaxation dispersion curves for T55 and V70, distributions of $R_2^{\beta,0}$ and R_2^0, measured values of R_1^β, values of μ_{1H} calculated from R_1 and R_2, R_2^β values measured using CRT experiments, and details of numerical simulations. This material is available free of charge via the Internet at http://pubs.acs.org.

References

(1) (a) Kern, D.; Zuiderweg, E. R. P. *Curr. Opin. Struct. Biol.* **2003**, *13*, 748−757. (b) Palmer, A. G. *Chem. Rev.* **2004**, *104*, 3623−3640. (c) Palmer, A. G.; Grey, M. J.; Wang, C. Y. *Methods Enzymol.* **2005**, *394*, 430−465.

(2) (a) Loria, J. P.; Rance, M.; Palmer, A. G. *J. Biomol. NMR* **1999**, *15*, 151−155. (b) Korzhnev, D. M.; Kloiber, K.; Kanelis, V.; Tugarinov, V.; Kay, L. E. *J. Am. Chem. Soc.* **2004**, *126*, 3964−3973.

(3) Wang, C. Y.; Rance, M.; Palmer, A. G. *J. Am. Chem. Soc.* **2003**, *125*, 8968−8969.

(4) Pervushin, K.; Riek, R.; Wider, G.; Wüthrich, K. *Proc. Natl. Acad. Sci. U.S.A.* **1997**, *94*, 12366−12371.

(5) Palmer, A. G.; Massi, F. *Chem. Rev.* **2006**, *106*, 1700−1719.

(6) Meissner, A.; Duus, J. O.; Sørensen, O. W. *J. Magn. Reson.* **1997**, *128*, 92−97.

(7) Sørensen, M. D.; Meissner, A.; Sørensen, O. W. *J. Biomol. NMR* **1997**, *10*, 181−186.

(8) Mulder, F. A. A.; de Graaf, R. A.; Kaptein, R.; Boelens, R. *J. Magn. Reson.* **1998**, *131*, 351−357.

(9) (a) Weigelt, J. *J. Am. Chem. Soc.* **1998**, *120*, 12706−12706. (b) Rance, M.; Loria, J. P.; Palmer, A. G. *J. Magn. Reson.* **1999**, *136*, 92−101.

(10) Kempf, J. G.; Jung, J. Y.; Sampson, N. S.; Loria, J. P. *J. Am. Chem. Soc.* **2003**, *125*, 12064−12065.

(11) Massi, F.; Johnson, E.; Wang, C. Y.; Rance, M.; Palmer, A. G. *J. Am. Chem. Soc.* **2004**, *126*, 2247−2256.

(12) Akke, M.; Palmer, A. G. *J. Am. Chem. Soc.* **1996**, *118*, 911−912.

(13) Sklenár, V.; Piotto, M.; Leppik, R.; Saudek, V. *J. Magn. Reson., Ser. A* **1993**, *102*, 241−245.

(14) Kroenke, C. D.; Loria, J. P.; Lee, L. K.; Rance, M.; Palmer, A. G. *J. Am. Chem. Soc.* **1998**, *120*, 7905−7915.

(15) Massi, F.; Grey, M. J.; Palmer, A. G. *Protein Sci.* **2005**, *14*, 735−742.

JA061692F